MIT
SEA
GRANT
PROGRAM

APPLICATION OF ESTIMATION THEORY TO DESIGN OF SAMPLING PROGRAMS FOR VERIFICATION OF COASTAL DISPERSION PREDICTIONS

by
Richard De Guida
Jerome J. Connor
Bryan Pearce

Massachusetts Institute of Technology

Cambridge, Massachusetts 02139

Report No. MITSG 76-16
November 20, 1976

APPLICATION OF ESTIMATION THEORY TO DESIGN OF SAMPLING PROGRAMS FOR VERIFICATION OF COASTAL DISPERSION PREDICTIONS

by

Richard De Guida
Jerome J. Connor
Bryan Pearce

Massachusetts Institute of Technology
Sea Grant Program

Report No. MITSG 76-16
Index No. 76-316-Ccb

Acknowledgements

This report was presented at the International Conference on Finite Elements in Water Resources, Princeton University, July 1976. The research was carried on as part of the M.I.T. Sea Grant Program with support from the Office of Sea Grant in the National Oceanic and Atmospheric Administration, U.S. Department of Commerce, through grant number 04-5-158-1, and from the Massachusetts Institute of Technology.

Related Reports

Parker, Bruce B., and Bryan R. Pearce. THE RESPONSE OF MASSACHUSETTS BAY TO WIND STRESS. MITSG 75-2. Cambridge: Massachusetts Institute of Technology. February 1975.

Lassiter, Joseph B., III, James E. Soden, and Robert J. Powers. AN ASSAY OF THE MARINE RESOURCES OF MASSACHUSETTS BAY. MITSG 74-26, NTIS COM-74-11589/AS. Cambridge: Massachusetts Institute of Technology, June 1974. 58pp. $2.50.

Christodoulou, Georgios C., William F. Leimkuhler, and Arthur T. Ippen. MATHEMATICAL MODELS OF THE MASSACHUSETTS BAY; PART III: A MATHEMATICAL MODEL FOR THE DISPERSION OF SUSPENDED SEDIMENTS IN COASTAL WATERS. MITSG 74-14, NTIS COM-74-10977/AS. Cambridge: Massachusetts Institute of Technology, January 1974. 143 pp. $4.00.

Note: The preceding publications may be ordered from the National Technical Information Service, U.S. Department of Commerce, Springfield, Virginia 22151. Use the NTIS number when ordering; prices are variable.

APPLICATION OF ESTIMATION THEORY TO DESIGN OF SAMPLING PROGRAMS FOR VERIFICATION OF COASTAL DISPERSION PREDICTIONS

Richard N. De Guida

Graduate Research Assistant, Department of Civil Engineering, M.I.T., Cambridge, Mass.

Jerome J. Connor

Professor, Department of Civil Engineering, M.I.T., Cambridge, Mass.

Bryan R. Pearce

Assistant Professor, Department of Civil Engineering, Cambridge, Mass.

INTRODUCTION

Experience and engineering judgment form the basic foundation for designing sampling programs. Collection of accurate field data is required for verification of constituent (pollutant) dispersion predictions. However, the complexity of the dispersal phenomenon precludes the design of optimal sampling strategies based upon only qualitative analyses; more substantial quantitative analyses are required.

The most informative sampling strategy would require the collection of samples covering the entire spatial and temporal domains of the particular problem at sufficiently small spatial and temporal intervals to ensure the identification of all important information. A greatly reduced number of samples is usually collected due to the imposition of cost constraints. In such cases, decisions must be reached as to which samples are, and which are not, to be collected. The importance of such decisions is magnified in short-term field sampling programs. In long-term monitoring programs, one has the capabil-

ity of altering the initial strategy to improve its effectiveness as data becomes available. Due to the relatively short duration of typical field sampling programs (e.g., tracer experiments), they must be designed before the start of the sampling effort, since the results of sampling are not usually available until after the commencement of the field program. Thus it is desirable that a methodology be made available to assist in the designing of effective sampling programs.

Only within the last few years have quantitative methodologies for determining spatial and temporal sampling intervals begun to appear in the technical literature. The particular methodology of interest is based upon the concepts of Estimation Theory (specifically, Kalman-Bucy filtering). Estimation Theory refers to a variety of statistical techniques developed for determining best approximations of unknown quantities from observations (data) which are recognized as being imperfect, i.e., containing uncertainty. Kalman-Bucy filtering is a technique available for the estimation of the states of a system by the sequential extraction of information from data, as the data becomes available. It has been employed successfully in the field of navigation and guidance of spacecraft since the mid 1960's, and several investigators have recently attempted to apply these concepts to environmental pollution problems. Moore [1973] applied filtering techniques to determine the minimum monitoring frequency of certain water quality constituents for a simulated river system. Brewer and Moore [1974] extended the work of Moore [1973] to include the problem of determining the water quality constituent to be sampled and their spatial locations. Although Desalu [1974] did not directly address the monitoring design problem, he illustrated the applicability of Estimation Theory to such air pollution problems as: i) estimation of the three-dimensional distribution of pollutant concentrations from observed data, ii) identification of the diffusion coefficient and other model parameters and iii) identification of the major sources of air pollution. Pimentel [1975] illustrated that a simplified formulation results when measurements are made infrequently. This approach required ignoring the advection of the constituent; only diffusion is considered, an assumption unsuitable for estuarine areas. In addition, the important question of what is the maximum rate of sampling that can be considered as infrequent was not addressed.

A common deficiency of the above studies is the lack of effort directed at quantifying the modeling uncertainty. Although filtering concepts are straightforward, difficulty arises in their application. A major difficulty is the quantification of the modeling uncertainty. Lettenmaier [1975] considers uncertainties in tributaries, waste sources and certain parameters in his approach to design of river monitoring programs

for detection of water quality trends. The use of a steady-state one-dimensional model and temporally constant uncertainty statistics severely restricts its usefulness. The work of Dandy [1976] appears to be the most complete study published to date. He considers the design of riverine monitoring programs using a one-dimensional transient model of the advection of water quality constituents. Modeling uncertainty due to randomly varying streamflow, tributary discharges, and waste sources is considered. However, he neglects constituent dispersion and model parameter uncertainties, and uses a simplified representation of the hydrodynamics.

In this paper, the analytical framework for applying Kalman-Bucy filtering to dispersion in a coastal water body is developed. Particular emphasis is placed on quantification of the model uncertainty due to model parameters, source loadings, and velocity fields. The formulation is discretized with the Finite Element Method, and a number of comparison studies are presented.

In what follows, we outline first the filtering strategy, then describe briefly the Finite Element implementation, and lastly discuss some examples.

FILTERING CONCEPTS

Consider a linear, discrete mathematical model of the following form:

$$\underline{X}(t+\Delta t) = \underset{\sim}{\Phi}(t)\underline{X}(t) + \underset{\sim}{\beta}(t)\underline{\Psi}(t) + \underline{\Omega}(t) \qquad (1)$$

where

- $\underline{X}$ is a n-dimensional system state vector
- $\underset{\sim}{\Phi}$ is a n x n dimensional state transition matrix
- $\underline{\Psi}$ is a n-dimensional vector of known deterministic inputs
- $\underset{\sim}{\beta}$ is a n x n dimensional factor matrix of the deterministic input vector
- $\underline{\Omega}$ is a n-dimensional vector of model uncertainty having zero mean and covariance $Q_{M_{(t)}}$, as designated by $(0, Q_{M_{(t)}})$
- $( )_{t+\Delta t}$ represents the array evaluated at time $t+\Delta t$
- $( )_t$ represents the array evaluated at time t
- Δt is the time increment

The state-space model form of Equation 1 allows the calculation of the system state vector at time $t + \Delta t$ from the system state vector at time t. Since $\underset{\sim}{\Phi}_{(t)}$ is independent of $\underline{X}_{(t)}$, the model is linear in the independent variable $\underline{X}_{(t)}$. It is also discrete, as opposed to continuous, since it allows the computation of the dependent system state vector at only discrete times (temporally

spaced Δt units of time apart). The deterministic model would not normally include the last term, $\underline{\Omega}_{(t)}$. It is included here to signify the uncertainty in the results predicted by the deterministic model. Specification of a zero mean model uncertainty defines an unbiased model. If the model is biased, and the value of the bias is known, the model uncertainty can be represented by a deterministic bias and a zero mean random contribution.

Consider next, the following linear, discrete form of the observations:

$$\underline{Z}_{(t)} = \underset{\sim}{H}_{(t)}\underline{X}_{(t)} + \underline{\gamma}_{(t)} \tag{2}$$

where

$\underline{Z}_{(t)}$ is a m-dimensional vector of field observations

$\underset{\sim}{H}_{(t)}$ is a m x n dimensional observation matrix

$\underline{\gamma}_{(t)}$ is a m-dimensional vector of observation uncertainty having zero mean and covariance $Q_{o_{(t)}}$, as designated by $(0, Q_{o_{(t)}})$

The observation matrix, $\underset{\sim}{H}_{(t)}$, designates the locations at which the data is collected. At each time step, a new observation matrix may be formulated, with the number of rows corresponding to the number of observations at that time. For each row, zeros (0's) appear in all columns except the column corresponding to a node of sampling; in this column, a one (1) is placed. For example, if only node 2 is measured in a 4 node system, the observation array will be:

$$[0 \quad 1 \quad 0 \quad 0]$$

Information from the model and observations can be combined by Kalman-Bucy filtering, as presented by Gelb [1974], Jazwinski [1970], and Schweppe [1973]. The first stage of the filter (i.e., prediction state) entails the extrapolation of both the state estimates and the system error covariances forward in time to the next discrete time point using the system model of Equation 1. Assuming that the model uncertainty is uncorrelated in time, the predicted system error covariance is:

$$\underset{\sim}{\Sigma}_{(t+\Delta t|t)} = \underset{\sim}{\Phi}_{(t)}\underset{\sim}{\Sigma}_{(t|t)}\underset{\sim}{\Phi}_{(t)}^{T} + \underset{\sim}{Q}_{M_{(t)}} \tag{3}$$

where

$\underset{\sim}{\Sigma}_{(t+\Delta t|t)}$ is a n x n dimensional predicted system error covariance matrix evaluated at time $t+\Delta t$, given measurements only up to and including time t.

$\underset{\sim}{\Sigma}_{(t|t)}$ is a n x n dimensional updated system error covariance matrix evaluated at time t, given measurements up to and including time t

The above expression emphasizes that the system uncertainties are propagated through the model in a way analogous to the system states themselves. The model error covariance, $Q_{M_{(t)}}$, arises due to the error introduced in the propagation of the system errors from one time step to the next by use of the model state transition matrix.

The updated system states are obtained from the predicted system states and a linear weighting of the difference between the predicted system values and the observations as:

$$\hat{\underline{X}}_{(t+\Delta t)} = \underline{X}_{(t+\Delta t)} + \underline{\underline{K}}_{(t+\Delta t)} \left[\underline{Z}_{(t+\Delta t)} - \underline{\underline{H}}_{(t+\Delta t)} \underline{X}_{(t+\Delta t)}\right] \quad (4)$$

where,

$\underline{X}_{(t+\Delta t)}$ is the n-dimensional vector of <u>updated</u> system states

Since minimum variance system state estimates are desired, that weighting function is computed which minimizes the trace of the predicted error covariance matrix. This weighting function, specifically called the Kalman gain matrix, is:

$$\underline{\underline{K}}_{(t+\Delta t)} = \underline{\underline{\Sigma}}_{(t+\Delta t|t)} \underline{\underline{H}}^{T}_{(t+\Delta t)} \left[\underline{\underline{H}}_{(t+\Delta t)} \underline{\underline{\Sigma}}_{(t+\Delta t|t)} \underline{\underline{H}}^{T}_{(t+\Delta t)} + Q_{o_{(t+\Delta t)}}\right]^{-1} \quad (5)$$

where

$\underline{\underline{K}}_{(t+\Delta t)}$ is the n x m dimensional Kalman gain matrix

$( )^{-1}$ indicates the inverse of the given array

$( )^{T}$ indicates the transpose of the given array

It is seen from Equation 5 that the Kalman gain matrix is computed from the weighting of the uncertainties in the predicted system values and the observations. With such, the updated system uncertainty is computed from:

$$\underline{\underline{\Sigma}}_{(t+\Delta t|t+\Delta t)} = \left[\underline{\underline{I}} - \underline{\underline{K}}_{(t+\Delta t)} \underline{\underline{H}}_{(t+\Delta t)}\right] \underline{\underline{\Sigma}}_{(t+\Delta t|t)} \quad (6)$$

where

$\underline{\underline{I}}$ is an n x n dimensional identity matrix

From the above, it is seen that the updated system error covariances can only be less than or equal to the predicted system error covariances. With perfect data, the system error covariances are reduced to zero at the locations of sampling. With uninformative data, the updated system error covariances will correspond exactly to the predicted system error covariances. An extremely important characteristic of the system error covariance update is its independence of the actual data values; only the statistics of the data uncertainty are required. This property allows the system error covariances to be computed before the data is made available, and thus, can be made to assist in the design of data collection programs.

To summarize the filtering process and computational requirements, the filter equations are presented in the flowchart of Figure 1. Whether data is available or not, the predicted system states and system error covariances must be calculated at each time step; the major computational cost of the filter is incurred here. In actuality, the computational difficulty and cost of filtering depends on whether the errors are white or colored (temporally invariant or correlated), and on whether the system is linear or nonlinear. The filtering algorithm presented here has made use of simplifying assumptions appropriate for linear system dynamics and temporally uncorrelated errors. For more detailed descriptions of filtering, the reader is referred to the works of Gelb [1974], Jazwinski [1970], and Schweppe [1973].

DETERMINISTIC DISPERSION MODEL

The deterministic model employed here is a vertically averaged two-dimensional finite element discretization which is applicable when the velocity and concentration vary slowly over the water column, i.e., for well mixed conditions. We have restricted the treatment to a vertically averaged formulation since our objective was to investigate the computational feasibility of applying filtering techniques and a three-dimensional treatment would be premature at this time.

Integrating the general convective diffusion equation over the water column results in the following governing equation (see Leimkuhler [1974] for details):

$$\frac{\partial}{\partial t} C + \frac{\partial}{\partial x} (\bar{u}\, C) + \frac{\partial}{\partial y} (\bar{v}\, C) = - \frac{\partial}{\partial x} Q_x - \frac{\partial}{\partial y} Q_y + \tilde{S}_i + \tilde{S}_s + \tilde{S}_b \qquad (7)$$

where

C is the depth integrated concentration,

$$C = \rho \bar{c}\, h$$

ρ is the mass density of the constituent and water mixture

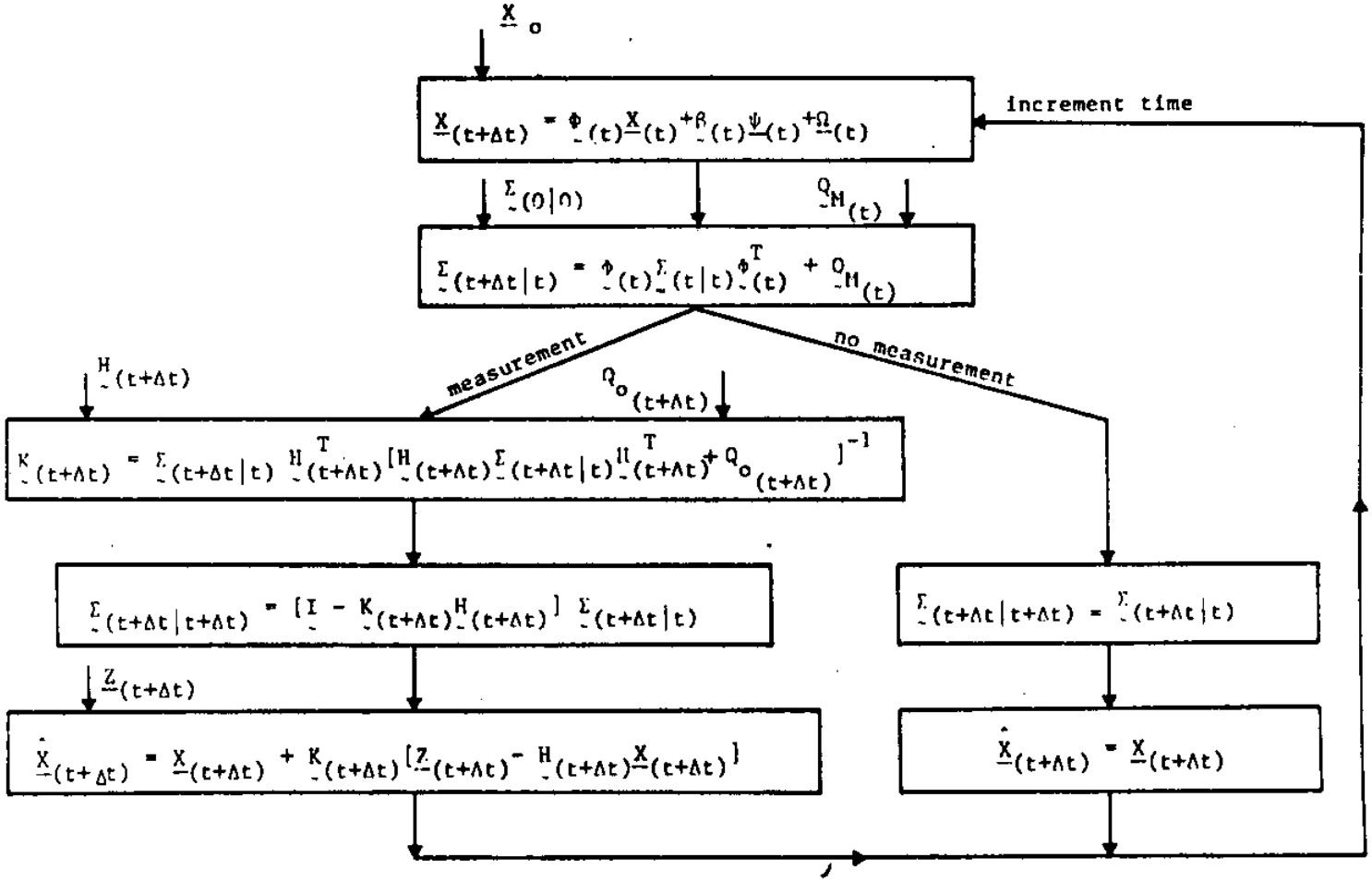

Figure 1 Schematic Diagram of Kalman Filtering Process

(from Pearce, et al. [1975])

$\bar{c}$, $\bar{u}$, $\bar{v}$ are the depth-averaged values of concentration and horizontal velocity components

h is the total height of water column

$\tilde{S}_i$ is the constituent mass input rate per unit projected area

$\tilde{S}_s$, $\tilde{S}_b$ are the normal source loading flux components through the surface and bottom of the water column

The flux terms are approximated with isotropic Fickian dispersion expressions,

$$Q_x = - \rho h E_{x,y} \frac{\partial \bar{c}}{\partial x} \tag{8}$$

$$Q_y = - \rho h E_{x,y} \frac{\partial \bar{c}}{\partial y} \tag{9}$$

where $E_{x,y}$ is the isotropic dispersion coefficient

For the particular case of settling of discrete particles (e.g., sphalerite tracer particles, suspended sediment, etc.), the source and sink terms are simplified by assuming a first order decay rate due to the settling velocity of the particles, and constant concentration through the layer. This yields

$$\tilde{S}_i + \tilde{S}_s + \tilde{S}_b = \tilde{S}_i - \rho w_s \bar{c} \tag{10}$$

where w_s is the particle settling velocity.

For coastal problems, the concentration is specified as C = 0 on the ocean boundary when the boundary is far from the plume. The normal dispersive flux is specified as $Q_n = 0$ along the land boundary. If the plume intersects the ocean boundary, the normal dispersive flux can be prescribed as being equal to zero provided that the concentration is constant outside the domain.

Equation (7) is transformed to its symmetrical weak form and the Finite Element spatial discretization is applied. The details are presented by Leimkuhler, et al (1975), and we list here only the final form of the governing equation:

$$\underset{\sim}{M} \frac{\partial}{\partial t} \underline{C} + \underset{\sim}{A} \cdot \underline{C} + E_{x,y} \cdot \underset{\sim}{K} \cdot \underline{C} + w_s \cdot \underset{\sim}{D} \cdot \underline{C} - \underline{S} + \underline{F} = 0 \tag{11}$$

where A contains the advective terms, $\underset{\sim}{K}$ defines the dispersion component, $\underset{\sim}{D}$ refers to decay, $\underline{S}$ contains the source loading, and $\underline{F}$ represents the dispersive boundary flux term.

The trapezium method is employed to propagate the solution in time. In the deterministic case, the scheme is relatively inexpensive since the state transition matrix, Φ, does not have to be generated. However, it is required for the covariance propagation If advection is treated with the "pure" trapezium, the generation of Φ would require matrix factorization at each time step. To reduce this effort, an Eulerian approximation for advection is introduced and the solution is propogated with

$$[\underset{\sim}{M} + \frac{\Delta t}{2}(E_{x,y} \cdot \underset{\sim}{K} + w_s \cdot \underset{\sim}{D})]\underline{C}_{n+1} = [\underset{\sim}{M} - \frac{\Delta t}{2}(E_{x,y} \cdot \underset{\sim}{K} + w_s \cdot \underset{\sim}{D}) - \Delta t \cdot \underset{\sim}{A}_n]\underline{C}_n + \frac{\Delta t}{2}(\underline{\hat{S}}_{n+1} + \underline{\hat{S}}_n) \quad (12)$$

where

$(\;)_n$ designates the given array evaluated at the discrete time point, t_n

Δt is the time increment

The Euler approximation for advection decreases the stability limit but this is usually not a problem for coastal dispersion.

QUANTIFICATION OF DISPERSION MODELING UNCERTAINTY

The major effort required in applying Kalman-Bucy filtering to coastal dispersion problems is quantification of the modeling uncertainty. Since coastal dispersion generally involves a large number of unknowns, only a first-order uncertainty analysis is feasible. In first-order analyses, each variable is considered to be a random function in which the mean represents the best estimate of the variable, and the variance quantifies the uncertainty in the estimate.

To compute the uncertainty in the predicted concentrations, due to parameter and input uncertainties, the deterministic model is expanded in a Taylor series about the mean values of the variables. Retaining only first-order terms, results in the following equation which defines the propagation of the uncertainty in concentration:

$$\left[\underset{\sim}{M} + \frac{\Delta t}{2}\left(E_{x,y} \cdot \underset{\sim}{K} + w_s \cdot \underset{\sim}{D}\right)\right] \tilde{\underline{C}}_{t+\Delta t}$$

$$= \left[\underset{\sim}{M} - \frac{\Delta t}{2}\left(E_{x,y} \cdot \underset{\sim}{K} + w_s \cdot \underset{\sim}{D}\right) - \Delta t \cdot \underset{\sim}{A}_t\right] \tilde{\underline{C}}_t$$

$$- \left[\frac{\Delta t}{2}\left(\tilde{E}^{x,y}_t \cdot \underset{\sim}{K} + \tilde{w}_{s_t} \cdot \underset{\sim}{D}\right) + \Delta t \cdot \tilde{\underline{A}}_t\right] \underline{C}_t$$

$$- \left[\frac{\Delta t}{2}\left(\tilde{E}^{x,y}_{t+\Delta t} \cdot \underset{\sim}{K} + \tilde{w}_{s_{t+\Delta t}} \cdot \underset{\sim}{D}\right)\right] \underline{C}_{t+\Delta t}$$

$$+ \frac{\Delta t}{2}\left[\left(\tilde{\underline{S}}\right)_t + \left(\tilde{\underline{S}}\right)_{t+\Delta t}\right] \qquad (13)$$

where $\tilde{(\ )}_t$ represents the uncertainty in the given variable at time t

Our representation of the model parameters and inputs is equivalent to considering the uncertainty about the mean value as a zero mean process. The isotropic dispersion coefficient and first-order decay rate uncertainties are interpreted as

$$\tilde{E}^{x,y} \sim (0, \sigma_E{}^2{}_{x,y})$$

$$\tilde{w}_s \sim (0, \sigma_{w_s}{}^2)$$

where σ_x^2 represents the variance of the uncertainty in the variable x

Representation of the model inputs uncertainty creates more difficulty. For multi-location source discharges, each discharge would normally have its own characteristic level of uncertainty. However, to simplify,the loading is expressed in terms of a single loading parameter and a vector defining the spatial distribution of the loading as,

$$\hat{\underline{S}}_t = \lambda_t \underline{R}_t$$

where

λ_t is the loading parameter

$\underline{R}_t$ is a vector describing the geographic locations of the loadings

If only one source location exists, such as in most tracer field experiments,the above expression is exact. The uncertainty in the loading parameter is represented as a random function with zero mean and prescribed variance,

$$\tilde{\lambda}_t \sim (0, \sigma_{\lambda_t}^2)$$

where $\tilde{\lambda}_t$ is the source loading uncertainty

$\sigma_{\lambda_t}^2$ is the variance of the source loading uncertainty

The flexibility of handling temporally and spatially variant velocity fields creates difficulty in representation of the advection field uncertainty. Our approach is based on formulating the uncertainty at the element level similar to the formulation of the element advection matrix of the deterministic dispersion model.

Equation 13 shows that the effect of velocity uncertainty on the uncertainty of the predicted model concentrations is determined from

$$[\underline{M} + \frac{\Delta t}{2} (E_{x,y} \cdot \underline{K} + w_s \cdot \underline{D})] \tilde{\underline{C}}_{t+\Delta t} = -\Delta t \cdot \tilde{\underline{A}}_t \cdot \underline{C}_t \qquad (14)$$

The advection uncertainty term is decomposed into influence matrices and vectors of the x and y component velocity field uncertainties as

$$-\Delta t \cdot \tilde{\underline{A}}_t \cdot \underline{C}_t = \underline{A}^{(u)}_t \cdot \tilde{\underline{u}}_t + \underline{A}^{(v)}_t \cdot \tilde{\underline{v}}_t \tag{15}$$

where $\tilde{\underline{u}}_t$ is the vector of x component velocity field uncertainties

$\tilde{\underline{v}}_t$ is the vector of y component velocity field uncertainties

Using Equations 14 and 15, the following factor matrices can be defined (details are presented in DeGuida [1976]):

$$\underline{\phi}_{u,t} = [\underline{M} + \frac{\Delta t}{2} (\underline{E}_{x,y} \cdot \underline{K} + w_s \cdot \underline{D})]^{-1} \cdot \underline{A}^{(u)}_t \tag{16}$$

$$\underline{\phi}_{v,t} = [\underline{M} + \frac{\Delta t}{2} (\underline{E}_{x,y} \cdot \underline{K} + w_s \cdot \underline{D})]^{-1} \cdot \underline{A}^{(v)}_t \tag{17}$$

Collecting the various uncertainty contributions, the two-dimensional model uncertainty expands to:

$$\begin{aligned} \tilde{\underline{C}}_{t+\Delta t} = {} & \underline{\phi}_{c,t+\Delta t} \tilde{\underline{C}}_t \\ & + \tilde{\underline{E}}^{x,y}_t \cdot \underline{\phi}_{E_{x,y},t} + \tilde{\underline{E}}^{x,y}_{t+\Delta t} \cdot \underline{\phi}_{E_{x,y},t+\Delta t} \\ & + \tilde{w}_{s_t} \cdot \underline{\phi}_{w_s,t} + \tilde{w}_{s_{t+\Delta t}} \cdot \underline{\phi}_{w_s,t+\Delta t} \\ & + \tilde{\lambda}_t \cdot \underline{\phi}_{\lambda,t} + \tilde{\lambda}_{t+\Delta t} \cdot \underline{\phi}_{\lambda,t+\Delta t} \\ & + \underline{\phi}_{u,t} \cdot \tilde{\underline{u}}_t + \underline{\phi}_{v,t} \cdot \tilde{\underline{v}}_t \end{aligned} \tag{18}$$

where

$$\underline{\phi}_{c,t+\Delta t} = [\underline{M} + \frac{\Delta t}{2} (\underline{E}_{x,y} \cdot \underline{K} + w_s \cdot \underline{D})]^{-1}$$

$$[\underline{M} - \frac{\Delta t}{2} (\underline{E}_{x,y} \cdot \underline{K} + w_s \cdot \underline{D}) - \Delta t \cdot \underline{A}_t]$$

$$\underset{\sim}{\phi}_{E_{x,y},t} = [\underset{\sim}{M} + \frac{\Delta t}{2}(E_{x,y} \cdot \underset{\sim}{K} + w_s \cdot \underset{\sim}{D})]^{-1} (-\frac{\Delta t}{2} \cdot \underset{\sim}{K} \cdot \underset{\sim}{C}_t)$$

$$\underset{\sim}{\phi}_{E_{x,y},t+\Delta t} = [\underset{\sim}{M} + \frac{\Delta t}{2}(E_{x,y} \cdot \underset{\sim}{K} + w_s \cdot \underset{\sim}{D})]^{-1}$$

$$(-\frac{\Delta t}{2} \cdot \underset{\sim}{K} \cdot \underset{\sim}{C}_{t+\Delta t})$$

$$\underset{\sim}{\phi}_{w_s,t} = [\underset{\sim}{M} + \frac{\Delta t}{2}(E_{x,y} \cdot \underset{\sim}{K} + w_s \cdot \underset{\sim}{D})]^{-1} (-\frac{\Delta t}{2} \cdot \underset{\sim}{D} \cdot \underset{\sim}{C}_t)$$

$$\underset{\sim}{\phi}_{w_s,t+\Delta t} = [\underset{\sim}{M} + \frac{\Delta t}{2}(E_{x,y} \cdot \underset{\sim}{K} + w_s \cdot \underset{\sim}{D})]^{-1}$$

$$(-\frac{\Delta t}{2} \cdot \underset{\sim}{D} \cdot \underset{\sim}{C}_{t+\Delta t})$$

$$\underset{\sim}{\phi}_{\lambda,t} = [\underset{\sim}{M} + \frac{\Delta t}{2}(E_{x,y} \cdot \underset{\sim}{K} + w_s \cdot \underset{\sim}{D})]^{-1} (\frac{\Delta t}{2} \cdot \underset{\sim}{R}_t)$$

$$\underset{\sim}{\phi}_{\lambda,t+\Delta t} = [\underset{\sim}{M} + \frac{\Delta t}{2}(E_{x,y} \cdot \underset{\sim}{K} + w_s \cdot \underset{\sim}{D})]^{-1} (\frac{\Delta t}{2} \cdot \underset{\sim}{R}_{t+\Delta t})$$

$\underset{\sim}{\phi}_{u,t}$ and $\underset{\sim}{\phi}_{v,t}$ are as defined in Equations 16 and 17.

The propagation of the variance is obtained by squaring the uncertainty and taking the expected value. The two-dimensional form is, assuming stationary random processes (i.e., time invariant statistics of the uncertainty) (see DeGuida [1976]):

$$\underset{\sim}{\Gamma}_{c,t+\Delta t} = \underset{\sim}{\phi}_{c,t+\Delta t} \underset{\sim}{\Gamma}_{c,t} \underset{\sim}{\phi}^T_{c,t+\Delta t}$$

$$+ \sigma^2_{E_{x,y}} [\underset{\sim}{\phi}_{E_{x,y},t} \underset{\sim}{\phi}^T_{E_{x,y},t} + \underset{\sim}{\phi}_{E_{x,y},t+\Delta t} \underset{\sim}{\phi}^T_{E_{x,y},t+\Delta t}$$

$$+ (\underset{\sim}{\phi}_{c,t+\Delta t} \underset{\sim}{\phi}_{E_{x,y},t} \underset{\sim}{\phi}^T_{E_{x,y},t}) + (\underset{\sim}{\phi}_{c,t+\Delta t} \underset{\sim}{\phi}_{E_{x,y},t} \underset{\sim}{\phi}^T_{E_{x,y},t})^T]$$

$$+ \sigma^2_{w_s} [\underset{\sim}{\phi}_{w_s,t} \underset{\sim}{\phi}^T_{w_s,t} + \underset{\sim}{\phi}_{w_s,t+\Delta t} \underset{\sim}{\phi}^T_{w_s,t+\Delta t}$$

$$+ \left(\underset{\sim}{\phi}_{c,t+\Delta t}\ \underset{\sim}{\phi}_{w_s,t}\ \underset{\sim}{\phi}^T_{w_s,t}\right) + \left(\underset{\sim}{\phi}_{c,t+\Delta t}\ \underset{\sim}{\phi}_{w_s,t}\ \underset{\sim}{\phi}^T_{w_s,t}\right)^T]$$

$$+ \sigma_\lambda^2\ [\underset{\sim}{\phi}_{\lambda,t}\ \underset{\sim}{\phi}^T_{\lambda,t} + \underset{\sim}{\phi}_{\lambda,t+\Delta t}\ \underset{\sim}{\phi}^T_{\lambda,t+\Delta t}$$

$$+ \left(\underset{\sim}{\phi}_{c,t+\Delta t}\ \underset{\sim}{\phi}_{\lambda,t}\ \underset{\sim}{\phi}^T_{\lambda,t}\right) + \left(\underset{\sim}{\phi}_{c,t+\Delta t}\ \underset{\sim}{\phi}_{\lambda,t}\ \underset{\sim}{\phi}_{\lambda,t}^T\right)^T]$$

$$+ \underset{\sim}{\phi}_{u,t}\ \underset{\sim}{\Gamma}_u\ \underset{\sim}{\phi}^T_{u,t} + \underset{\sim}{\phi}_{v,t}\ \underset{\sim}{\Gamma}_v\ \underset{\sim}{\phi}^T_{v,t} \qquad (19)$$

where

$\underset{\sim}{\Gamma}_{c,t}$ is the variance of the model predicted concentrations at time t

$\underset{\sim}{\Gamma}_u$ is the variance of the x-directional depth averaged velocity components

$\underset{\sim}{\Gamma}_v$ is the variance of the y-directional depth averaged velocity components

SAMPLING EFFECTIVENESS DETERMINATION

Once the modeling uncertainty is quantified, a Kalman filtering algorithm is developed to quantify the effectiveness of sampling, as has been shown by previous investigators (e.g., Moore (1973), Brewer and Moore (1974), Pimentel (1975), and Dandy (1976)). With Kalman filtering, all that needs to be specified for the update of the system uncertainty are the observation matrices defining the locations of measurements in time and the statistics of the uncertainty in those measurements. If an estimate of the measurement uncertainty is available, the system uncertainty can be propagated in time, considering different observation matrices, i.e., different sampling strategies. Comparing the system uncertainty allows one to evaluate the potential effectiveness of various sampling strategies before the actual experiment is performed.

In designing sampling strategies by Kalman filtering, careful analysis is required in defining the observation matrices. The formulation as stated is entirely general, such that an infinite number of possible sampling networks (i.e., definition of the time-variant spatial locations of sampling) can be analyzed, if so desired. However, specific characteristics of each problem will normally limit the possible number

of sampling strategies to be tested. Of concern might be such factors as budgets allotted for sampling, required level of information from sampling, restricted sampling days and/or hours of sampling (e.g., only sunlight hours), political boundaries, certain legal aspects, and so on. All these factors, and many more, will probably influence the selection of possible sampling strategies. Of extreme importance here is the use of experience in sampling and engineering judgment.

For observations to be informative, the uncertainty of the observations must be less than the uncertainty in the predicted concentrations, i.e., the updated system uncertainty must be less than the predicted system uncertainty. It is therefore natural to choose the sampling strategy of minimum system uncertainty (i.e., the minimum system error covariance matrix). However, as the duration of time increases after the last observation has been made, the system uncertainty increases until finally no reduction in the system uncertainty is noticed. Therefore, at different times, different measures of the effectiveness of sampling would be obtained. To compute the sampling effectiveness over the entire time duration of the experiment, the reduction in the system error covariance matrix (i.e., predicted system error covariance matrix minus updated system error covariance matrix) is calculated at each time a sample is collected. Since the majority of the reduction occurs in the uncertain variances (i.e., diagonal elements of the system error covariance matrix), only the reductions in the trace are computed. Summation over time of these component reductions leads to a total measure of sampling effectiveness. Maximization of the total reductions of the system uncertainty is therefore an appropriate measure of sampling effectiveness for the specific problem of tracer experiments.

Some may criticize the previously described optimality criterion for the simplistic way of defining the feasible set of sampling strategies, i.e., observation matrices. In reality, even though a particular sampling strategy may not satisfy all the constraints, the penalty incurred in the constraint violation may be so small that the design will be more effective than all the others tested which satisfy the imposed constraints. These problems can be avoided by the definition of a utility function which could be made to reflect the value of sampling in light of all the complicating factors. The criterion for determining the most effective sampling network would be that network which maximizes the expected utility. Such a maximization of the expected utility has become a traditional objective in Bayesian statistical decision theory.

A major disadvantage of defining the sampling effectiveness as

maximization of the expected utility is the difficulty of expressing the utility in mathematical form. It is often very difficult to quantify certain characteristics of the problem; it may be practically feasible for only very special cases. Therefore, in light of the necessity to develop simpler evaluation criteria, evaluation of only feasible sampling strategies, as previously described, appears to be the most appropriate for the purposes of this study.

RESULTS

For purposes of illustrating the usefulness of the filtering algorithm for evaluating sampling effectiveness, some results for the one-dimensional modeling of a channel are presented first. The finite element grid used is shown in Figure 2. A constant depth of 1 meter is used. Contaminant is continuously injected at the source node. Zero concentrations are specified at the extreme ends of the grid (i.e., at $x = 0$ and $x = 3$ meters). A time increment of 0.1 seconds is used in the model. The mean values and standard deviations of the model parameters and inputs are:

Parameter	Mean Value	Standard Deviation
longitudinal dispersion coefficient	0.01 meters^2/sec	0.005 meters^2/sec
first order decay rate	0.2/sec	0.1/sec
Input		
longitudinal flow velocity	0.05 meters/sec	0.01 meters/sec
continuous source loading rate	1 gram/sec	0.1 gram/sec

In addition, the standard deviation of the measurement uncertainty is taken as 0.01 grams/meter^3.

Examination of the deterministic solution shows that the peak concentration occurs at the source location. Therefore, the first sampling strategy evaluated consisted of sampling at the source discharge location (node 9 in Figure 2) every second after the start of discharge. Since the trace of the error covariance matrix is the desired measure of sampling effectiveness, a plot of the trace of the error covariance matrix versus time is presented in Figure 3. The solid line in the

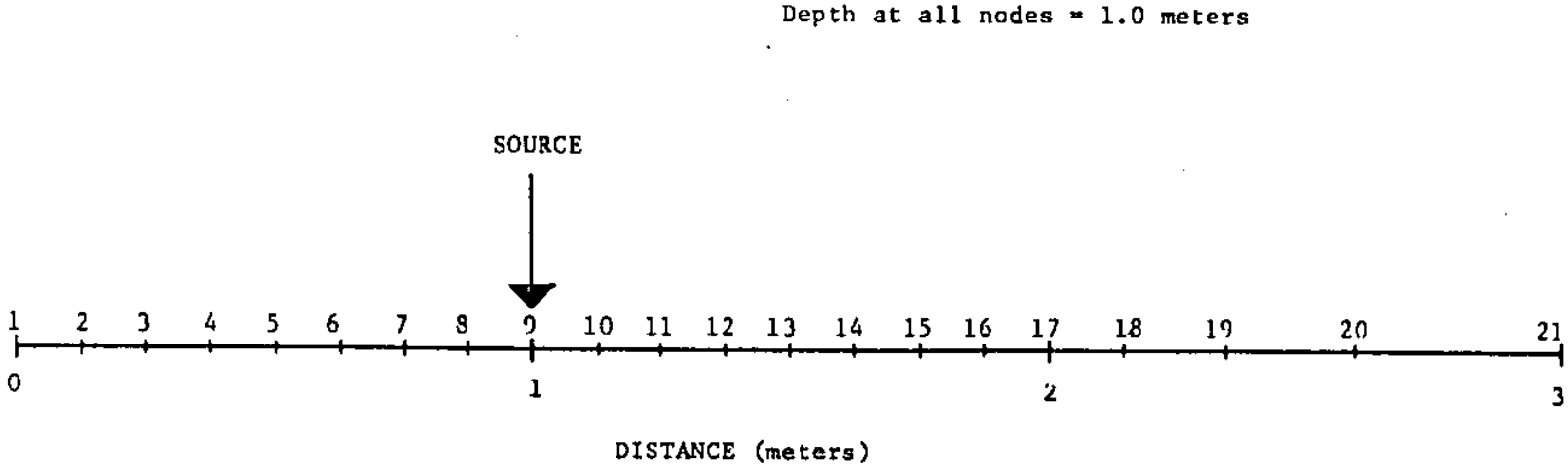

Figure 2 Finite Element Grid Used for One-dimensionnl Dispersion Model Simulations

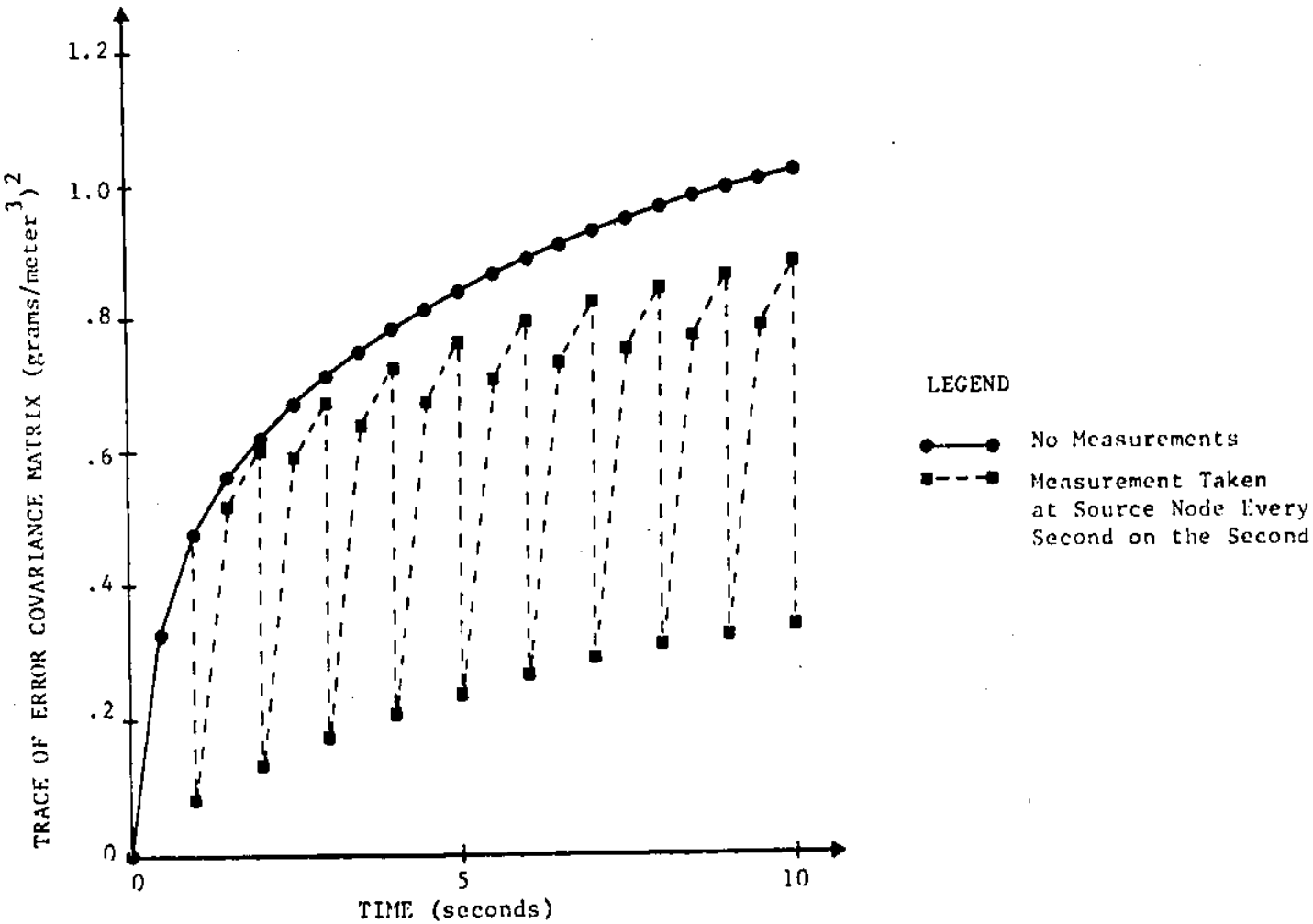

Figure 3 Temporal Effect of Sampling at Source Node Every Second

figure represents the modeling uncertainty (i.e., system uncertainty with no measurements); the dashed line represents the system uncertainty as measurements are taken. Each measurement reduces the system uncertainty at the time of measurement. However, as time progresses, the system uncertainty increases, but not quite to the level corresponding to no measurement. This indicates that the measurements are informative. A measure of their value is the total reduction in system uncertainty over time.

Figure 4 shows the variation of system uncertainty with distance from the source. The solid line defines the standard deviation of the system uncertainty immediately before the measurement is taken at 10 seconds; the dashed line is the "corrected" distribution. The effect of the measurement is quite local, reducing the system uncertainty to essentially the measurement uncertainty at the observation point but diminishing rapidly away from the source.

Figure 5 illustrates the effect of sampling every second after the start of discharge at the source node and half a meter downstream (i.e., nodes 9 and 13), as measured by the trace of the error covariance matrix. Figure 6 shows the reduction of the system uncertainty as a function of distance from the source at 10 seconds after start of discharge. The additional downstream observation point reduces the covariance trace, and also increases the spatial extent of the correction. The effect of increasing the sampling frequency while sampling at only the source node is illustrated by comparing Figures 3 and 7. Figure 7 illustrates the effect of taking a sample every half second.

Considerable interest in the Massachusetts Bay environment has been expressed in connection with a once proposed offshore sand and gravel dredging project called NOMES (New England Offshore Mining Environmental Study). Such interest has motivated this study, and it seemed logical to attempt a simulation of the NOMES dispersion experiment.

The finite element grid of Massachusetts Bay is shown in Figure 8. The ability to use elements of different sizes and shapes affords the flexibility required to model such complex geometric configurations as Massachusetts Bay. The dump site of tracer particles (sphalerite) is indicated by the starred area. Depths at the nodal points are taken from the Coast and Geodetic Survey bathymetric chart 0808N-50.

Velocity time histories were generated with a two-dimensional finite element circulation model, CAFE (Circulation Analyses by Finite Elements) (see Wang and Connor [1975]) using simulated tidal input and actual wind conditions collected during

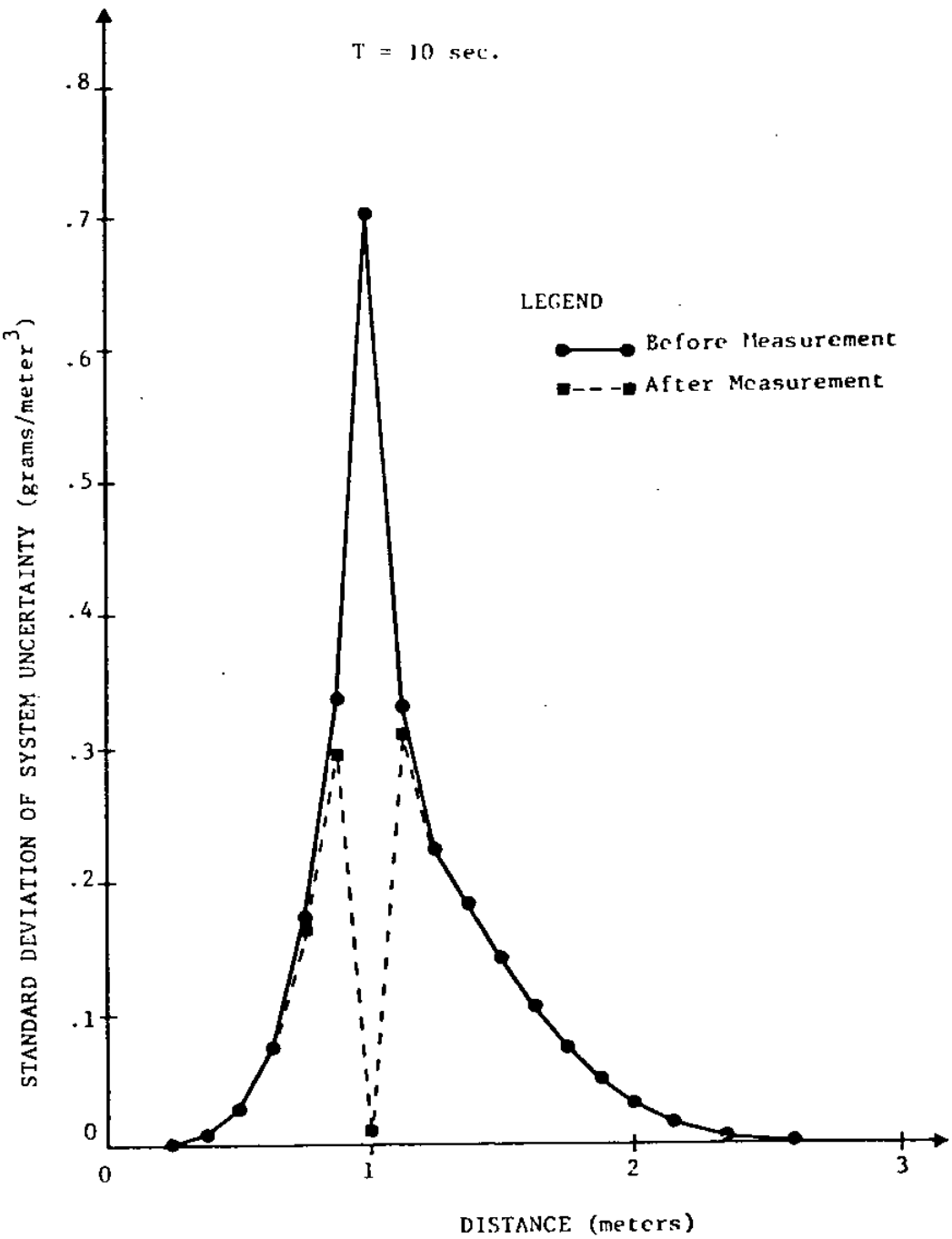

Figure 4 Spatial Effect of Sampling at Source Node for T = 10 Seconds

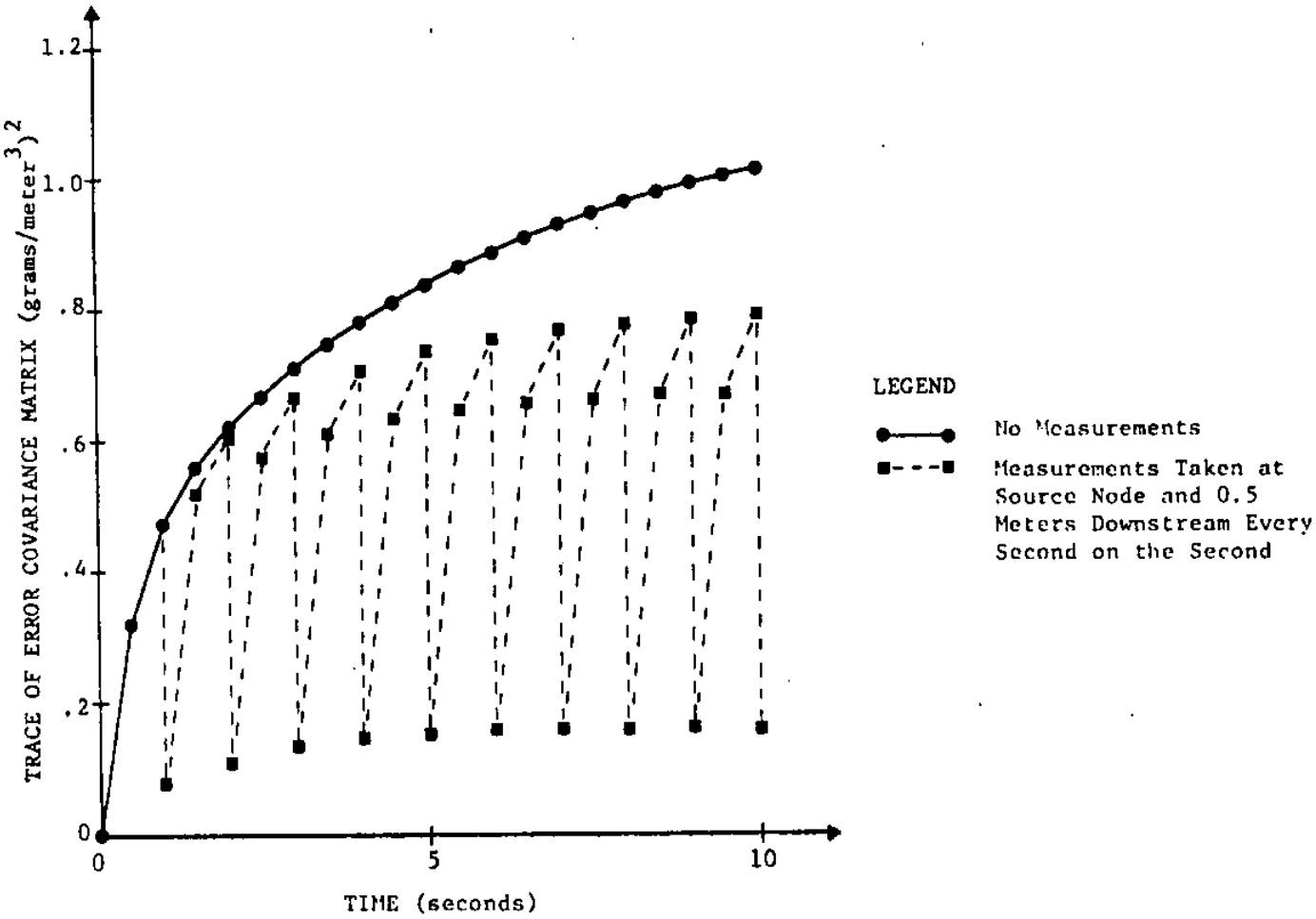

Figure 5 Temporal Effect of Sampling at Source Node and 0.5 Meters Downstream Every Second

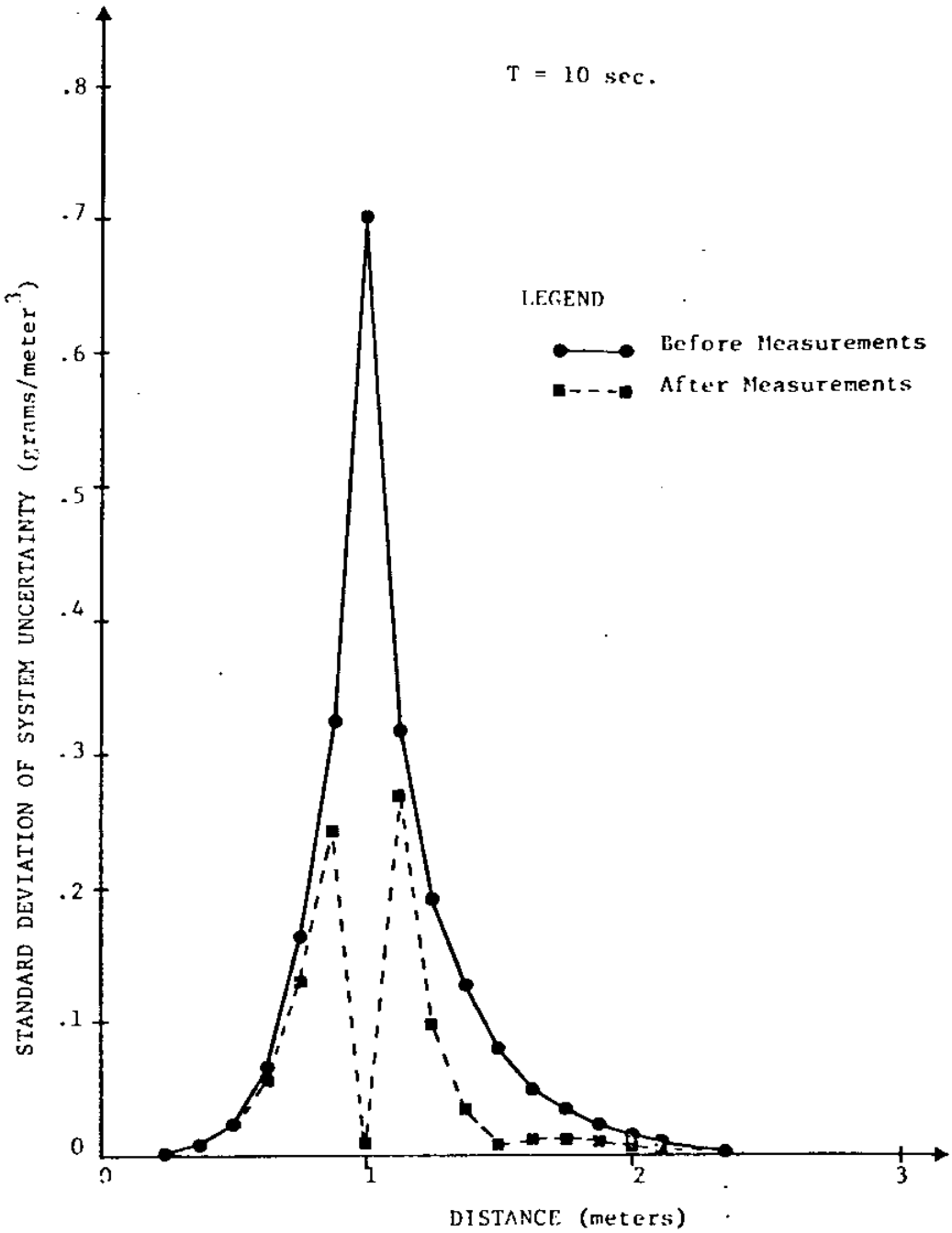

Figure 6 Spatial Effect of Sampling at Source Node and 0.5 Meters Downstream for T = 10 seconds

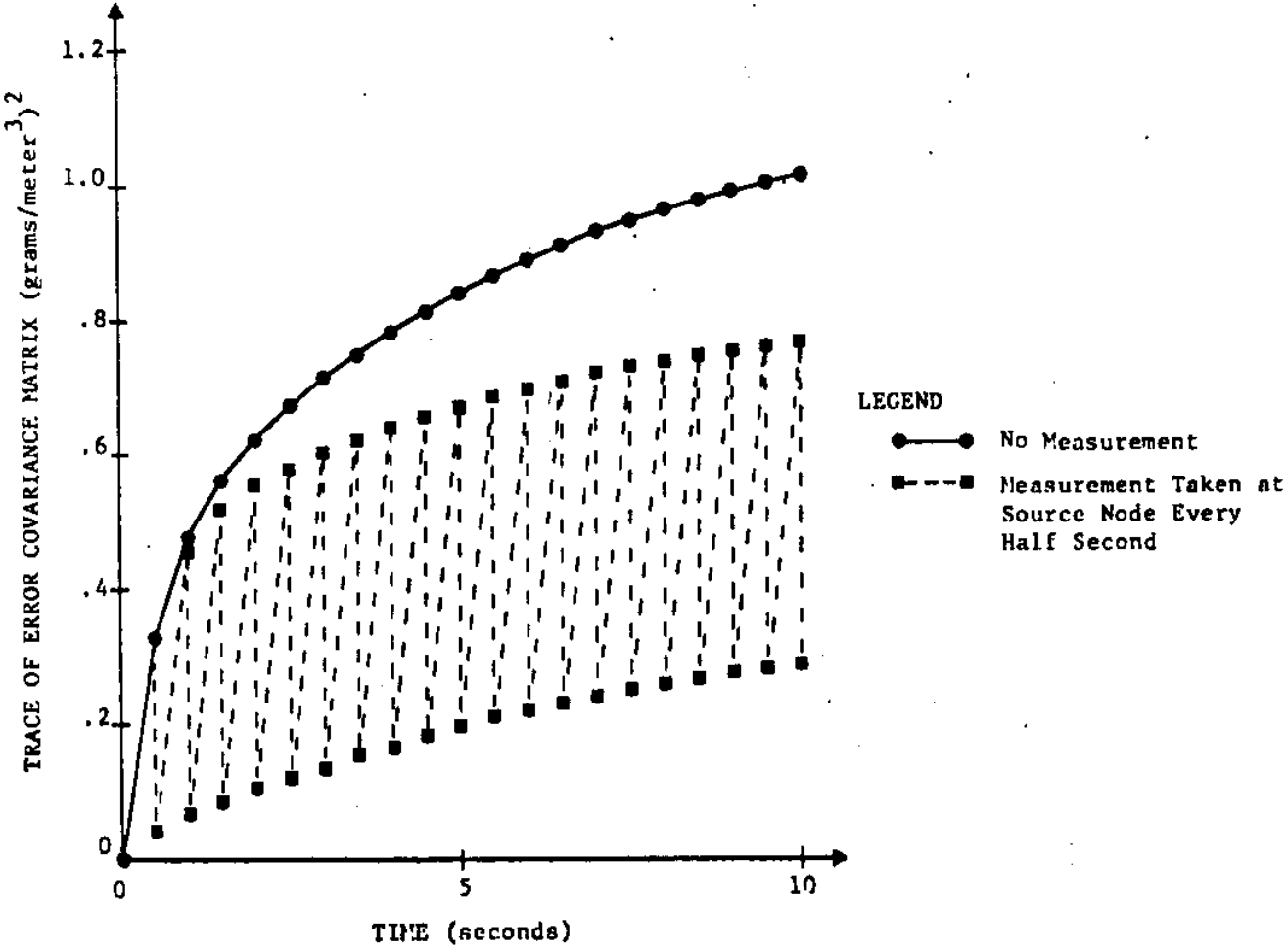

Figure 7 Temporal Effect of Sampling at Source Node Every Half Second

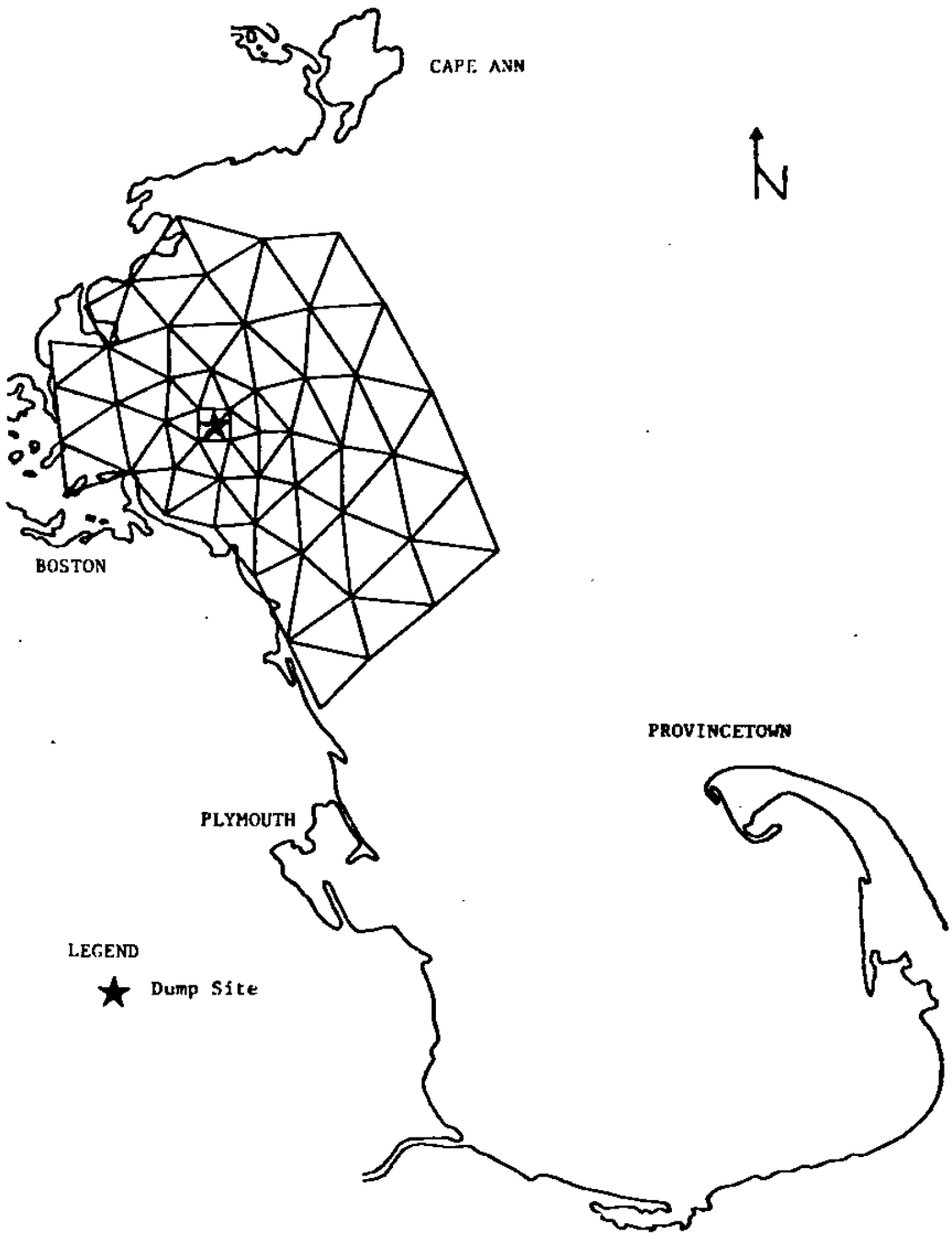

Figure 8 Finite Element Grid of Massachusetts Bay

the time period of the experiment.

In the NOMES experiment, approximately 1200 lbs. of sphalerite particles (mean diameter of approximately 5 microns; estimated 2.9×10^{15} particles) were dumped in a small area to simulate a point source discharge. Discharge began approximately one hour before low tide and lasted for approximately 10 minutes. Certain approximations are required in the mathematical modeling of the discharge. In the numerical simulation, it is necessary to take the duration of discharge equal to at least one time increment. (The time increment used in the dispersion model is 900 seconds.) In addition, although the discharge was essentially a point source, the source has to be distributed over a larger area (starred in Figure 8) in order to reduce the high concentration gradients which introduce numerical difficulties. In addition, the finite element grid is refined in the general discharge area for the same reason. Due to the spreading of the source over larger spatial and temporal scales, initial spreading is expected to be greater for the numerical results than in the actual experiment. With increasing time, this discrepancy should vanish.

The first order decay rate due to particle settling is obtained from Stoke's Law and assuming a uniform concentration profile over the water column depth as 3.3×10^{-5} meters/sec. The isotropic dispersion coefficient is chosen as 30 meters^2/sec (Pearce and Christodoulou [1975]).

Sensitivity of the dispersion model to uncertainty in the dispersion coefficient is addressed. Taking the standard deviation of the isotropic dispersion coefficient as 50% of the mean value (i.e., $\sigma_{E^{x,y}} = 15$ meters^2/sec), the effect on the predicted concentrations is shown in Figure 9 for a time of 12 hours after dump. Since dispersion is influenced by the concentration gradient, larger concentration uncertainties are expected in regions of steep concentration gradients. This is confirmed by the results shown.

Figure 10 illustrates the model sensitivity to a standard deviation of the decay rate equal to 50% of the mean value (i.e., $\sigma_{w_s} = 1.65 \times 10^{-5}$ meters/sec) at a time of 30 hours after dump. The model is observed to be less sensitive to a 50% of mean value standard deviation of the decay rate uncertainty than the dispersion uncertainty. The largest effect of the decay rate uncertainty is observed at the highest concentrations, as is expected.

The extent of application of the filtering algorithm for quantifying sampling effectiveness at the NOMES site was severely restricted by the high computational cost. For

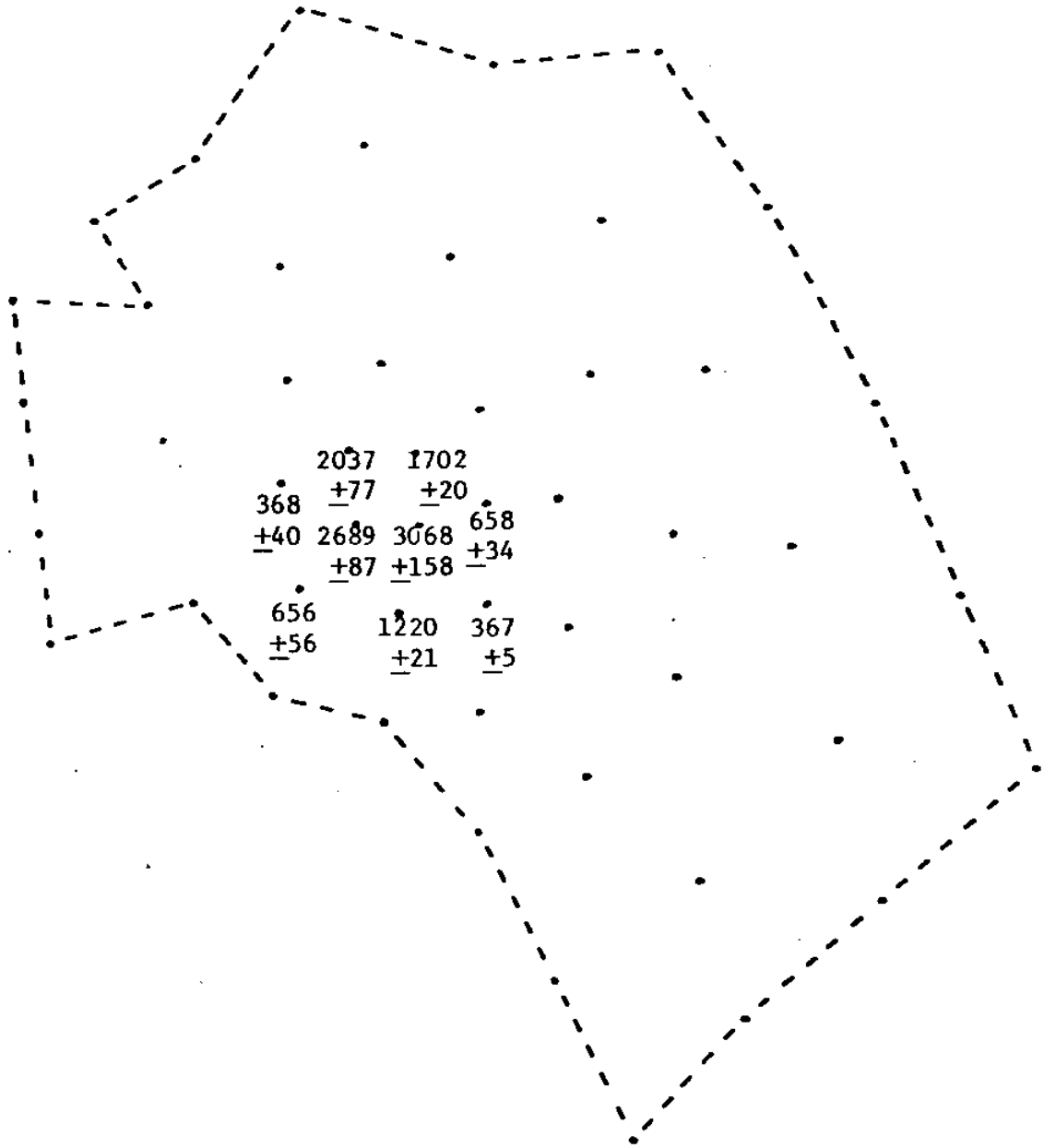

Figure 9 Mean Particle Concentrations and Standard Deviations of Modeling Uncertainty from a 15 meter^2/sec Standard Deviation of the Dispersion Coefficient at 12 Hours After Dump (particles/liter)

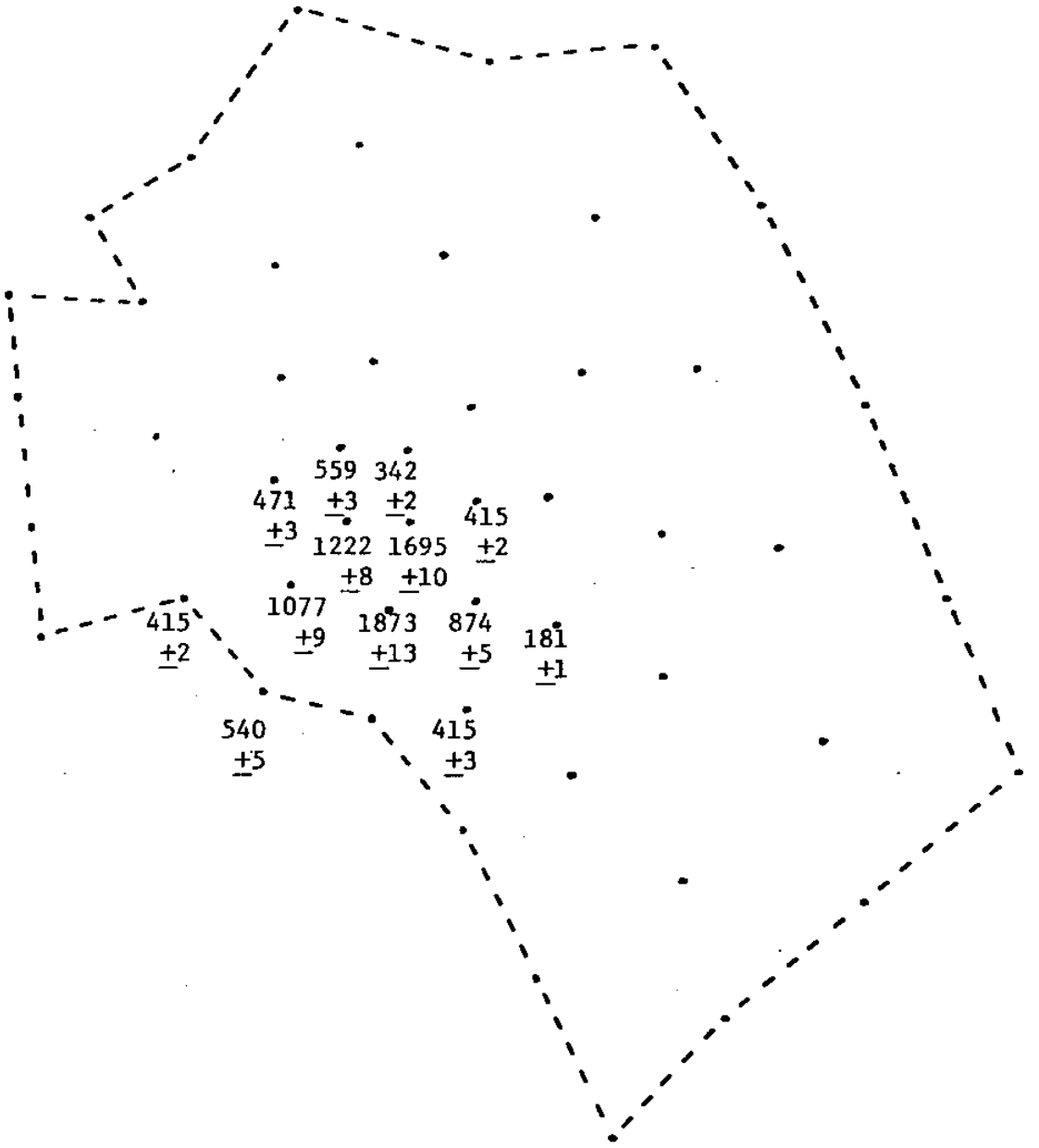

Figure 10 Mean Particle Concentrations and Standard Deviations of Modeling Uncertainty from a 1.65×10^{-5} meter/sec Standard Deviation of the Decay Rate at 30 Hours After Dump (particle/liter)

simulating the experiment for two full prototype days, the 50 state variable problem (see Figure 8) is required, but the computational problem is much too large for extensive simulation.

Given computational cost constraints, only one hypothetical sampling strategy was evaluated. Sampling was initiated at 9:00a.m. on the day following the dump (i.e., corresponding model time step 88). Samples were collected at the model source loading nodes every hour, until the completion of the sampling day at 4:00p.m. (i.e., corresponding to model time step 116). For purposes of presentation, the modeling uncertainty was computed from the uncertainty in the decay rate only. Figure 11 illustrates the effectiveness of the defined sampling strategy. In this figure, one observes the reduction in the system uncertainty due to the sampling effort. An interesting result is the very slow increase of the system uncertainty after the completion of sampling. Unfortunately, due to computational cost constraints, it was not possible to calculate the time duration after which no effect of the sampling would be felt.

CONCLUSIONS

Although a limited computer budget restricted the application to the NOMES experiment in Massachusetts Bay, these applications and extensive applications of the one-dimensional formulation have provided useful information on its computational costs and applicability.

The assessment of sampling effectiveness is made possible by filtering techniques. It allows the investigation of altered spatial and temporal frequency of sampling. However, the methodology does have limitations. One of the most critical is the requirement of the state-space representation of the system dynamics. Models are not generally developed in this form, due to the computational efficiency of other solution forms and the non-intuitive nature of the state-space form.

Although computation of the modeling uncertainty due to uncertainty in the dispersion coefficient, decay rate, velocity field, and source loading is presented, other uncertainty sources are not included. Uncertainty arises from assumptions made in the model formulation itself, which is difficult to quantify. For example, models are imperfect due to the assumptions of the applicability of Fickian diffusion and representation of naturally variant three-dimensional water bodies by lower dimensional models. Physical discretization

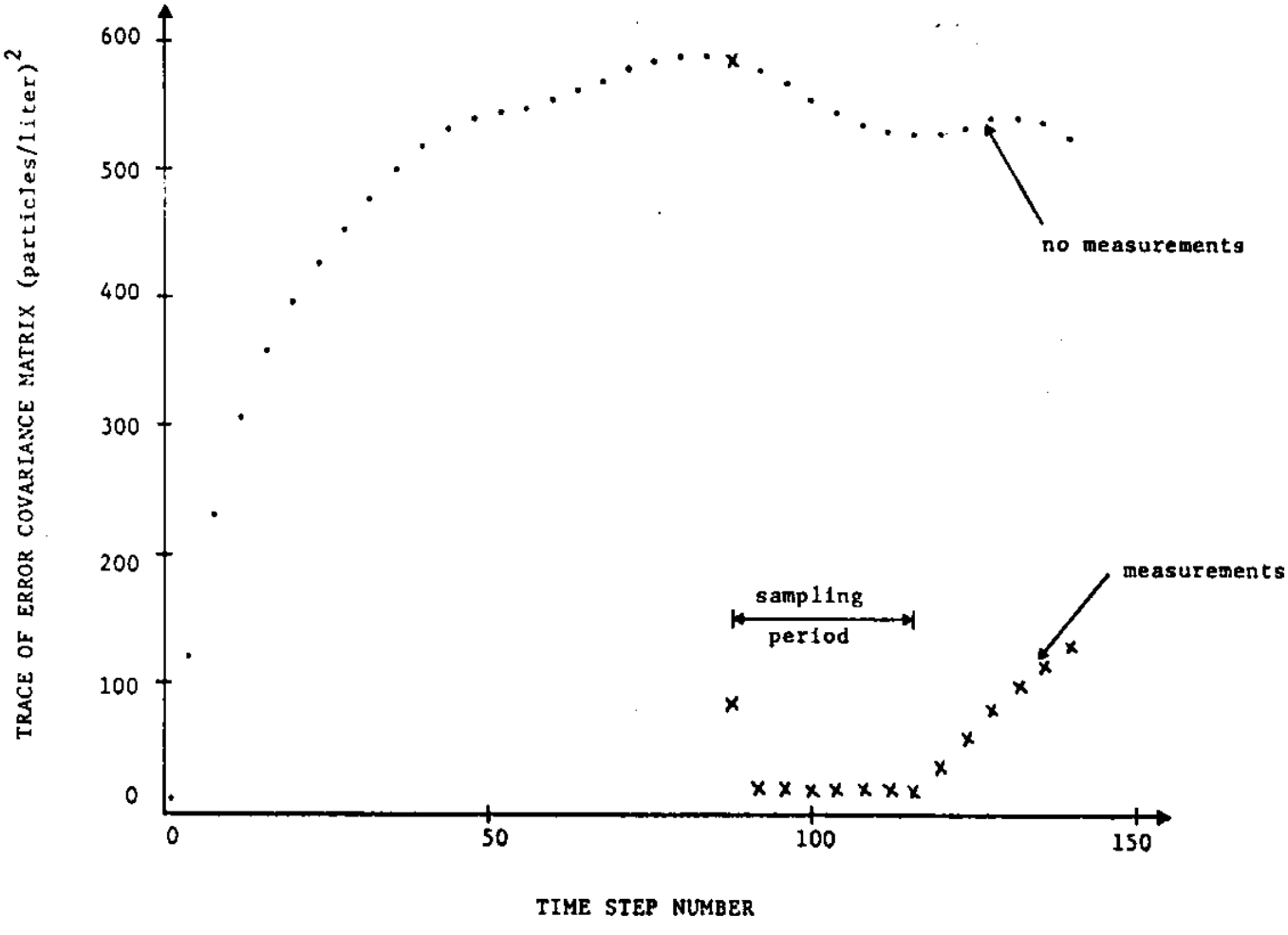

Figure 11 Temporal Effect of Hypothetical Sampling Strategy

of the continuous problem, both spatially and temporally, introduces numerical errors. By refining the grid and reducing the time increment, more accurate results are obtained, but at the expense of increased computational costs. In addition, round-off error can have significant effect on modeling results, but unfortunately has not received much attention.

The major reason for not including the effect on the modeling uncertainty of the above factors is the increased computational cost required. As is, calculation of the modeling uncertainty due to uncertainty in the parameters and inputs is costly for large systems. Calculation of the one-dimensional modeling uncertainty took roughly about 2 minutes of CPU time on an IBM 370 model 168 computer for a simulation of 21 nodes for 100 time steps. In comparison, calculation of the two-dimensional modeling uncertainty in application to Massachusetts Bay (neglecting uncertainty in the velocity field) took roughly 90 minutes of CPU time on the same computer for a simulation of 50 nodes for 144 time steps. Therefore, for large systems, the cost of computing the modeling uncertainty does become excessive; the additional cost of the Kalman filtering algorithm is insignificant.

An especially important conclusion of this study is the necessity to quantify the modeling uncertainty by a relatively detailed analysis. Many previous investigators (e.g., Moore (1973), Brewer and Moore (1974) and Pimentel (1975)) have obtained constant values of the modeling uncertainty based strictly upon subjective judgment. This practice is not advisable, as this work has shown the large spatial and temporal variability of the modeling uncertainty.

The tradeoff between computational cost and accuracy in quantifying the modeling uncertainty is evident. For simplistic one-dimensional modeling attempts, the relatively low computational cost justifies detailed modeling uncertainty analyses. The modeling uncertainty due to model assumptions, physical discretizations, round-off error, etc., should be addressed. On the other hand, difficulty in justifying the excessive computational costs of two-dimensional modeling of a Massachusetts Bay size problem exists. Although it is felt that the investment made in the simulation of a field experiment before it is actually performed will pay for itself in the higher return of information, the initial capital outlay for computational time may deter the use of such a methodology. Cheaper methods of calculating the modeling uncertainty are needed.

ACKNOWLEDGEMENTS

The research reported on in this paper was supported by the National Oceanographic and Atmospheric Administration Office of Sea Grant, Department of Commerce, through the M.I.T. Sea Grant Office.

REFERENCES

1. Brewer, J.W. and S.F. Moore, "Monitoring: An Environmental State Estimation Problem," ASME Journal of Dynamic Systems, Measurement and Control, pp. 363-365, 1974.

2. Dandy, G.C., "Design of Water Quality Sampling Systems for River Networks," Doctor of Philosophy Thesis, Department of Civil Engineering, Massachusetts Institute of Technology, June 1976.

3. DeGuida, R.N., "Design of Effective Sampling Programs for Verification of Coastal Dispersion," Master of Science Thesis, Department of Civil Engineering, Massachusetts Institute of Technology, May 1976.

4. Desalu, A.D., "Dynamic Air Quality Estimation in a Stochastic Dispersive Atmosphere," Doctor of Philosophy Thesis, Department of Electrical Engineering, Massachusetts Institute of Technology, April 1974.

5. Gelb, A.(Editor), Applied Optimal Estimation, M.I.T. Press, Massachusetts Institute of Technology, Cambridge, Massachusetts, 1974.

6. Jazwinski, A.H., Stochastic Processes and Filtering Theory, Academic Press, New York, 1970.

7. Leimkuhler, W.F., "A Two-Dimensional Finite Element Dispersion Model," Engineer's Thesis, Department of Civil Engineering, Massachusetts Institute of Technology, September 1974.

8. Leimkuhler, W.F., Connor, J.J., Wang. J.D., Christodoulou, G.C., and Sundgren, S.L., "A Two-Dimensional Finite Element Dispersion Model," Proceedings of the Symposium on Modeling Techniques for Waterways, Harbors and Coastal Engineering, San Francisco, California, September 1975.

9. Lettenmaier, D.P., "Design of Monitoring Systems for Detection of Trends in Stream Quality." Technical Report No. 39, Charles W. Harris Hydraulics Laboratory, Seattle, Washington, August 1975.

10. Moore, S.F., "Estimation Theory Applications to Design of Water Quality Monitoring Systems," Journal of Hyd. Div., ASCE, HY5, pp. 815-831, May 1973.

11. Pearce, B.R. and Christodoulou, G.C., "Application of a Finite Element Dispersion Model for Coastal Waters," Proceedings XVI IAHR Congress, Sao Paulo, Brazil, July 1975.

12. Pearce, B.R., De Guida, R.N., Dandy, G.C. and Moore, S.F., "Sampling Network Design for Dispersion Verification," Proceedings of the Symposium on Modeling Techniques for Waterways, Harbors and Coastal Engineering, San Francisco, California, September 1975.

13. Pimentel, K.D., "Toward a Mathematical Theory of Environmental Monitoring: The Infrequent Sampling Problem," Ph.D. Thesis, University of California, Livermore, June 1975.

14. Schweppe, F.C., Uncertain Dynamic Systems, Prentice-Hall, Inc., Englewood Cliffs, New Jersey, 1973.

15. Wang, J.D. and Connor, J.J., "Mathematical Modeling of Near Coastal Circulation," Technical Report No. 200, R.M. Parsons Laboratory for Water Resources and Hydrodynamics, Department of Civil Engineering, Massachusetts Institute of Technology, April 1975.